Further evidence in favour of a carbanion mechanism for glycolate oxidase

Hélène Pasquier, Florence Lederer

FEBS openbio

FEBS PRESS science publishing by scientists

RESEARCH ARTICLE

Further evidence in favour of a carbanion mechanism for glycolate oxidase

Hélène Pasquier and Florence Lederer

CNRS UMR 8000, Faculté des Sciences, Institut de Chimie Physique, Université Paris-Saclay, Orsay, France

Keywords
carbanion; chemical mechanism; glycolate oxidase; lactate; trifluorolactate

Correspondence
F. Lederer, CNRS UMR 8000, Faculté des Sciences, Institut de Chimie Physique, Université Paris-Saclay, Orsay 91405, France
E-mail: florence.lederer@universite-paris-saclay.fr

(Received 28 June 2022, revised 1 November 2022, accepted 11 December 2022)

doi:10.1002/2211-5463.13534

The flavoenzyme glycolate oxidase oxidizes glycolic acid to glyoxylate and the latter, more slowly, to oxalate. It is a member of an FMN-dependent enzyme family that oxidizes L-2-hydroxy acids to keto acids. There has been a controversy concerning the chemical mechanism of substrate oxidation by these enzymes. Do they proceed by hydride transfer, as observed for NAD-dependent enzymes, or by initial formation of a carbanion that transfers the electrons to the flavin? The present work describes a comparison of the reactivity of glycolate, lactate and trifluorolactate with recombinant human glycolate oxidase, by means of rapid-kinetics experiments in anaerobiosis. We show that trifluorolactate is a substrate for glycolate oxidase, whereas it is known as an inhibitor for NAD-dependent enzymes, as is trifluoroethanol for NAD-dependent alcohol dehydrogenases. Unexpectedly, it was observed that, once reduced, a flavin transfers an electron to an oxidized flavin, so that the end species is a flavin semiquinone, whatever the substrate. This phenomenon has not previously been described for a glycolate oxidase. Altogether, considering that another member of this flavoenzyme family (flavocytochrome b_2, a lactate dehydrogenase) has also been shown to oxidize trifluorolactate (Lederer F et al. (2016) Biochim Biophys Acta 1864, 1215–21), this work provides another important piece of evidence which is hardly compatible with a hydride transfer mechanism for this flavoenzyme family.

The peroxisomal flavoenzyme glycolate oxidase (EC1.1.3.15, isozyme A, also called short-chain hydroxy acid oxidase or HAOX1) is present in plants and animals. The tetrameric enzyme catalyses the oxidation of glycolate to glyoxylate at the expense of oxygen and, more slowly, of hydrated glyoxylate to oxalate [1,2]. In plant leaves, it is involved in the photorespiratory cycle. Among plant glycolate oxidases, the spinach one (sGOX) has been the best studied at the molecular level, with kinetic characterizations of the wild-type and variant enzymes, and determination of crystal structures with and without inhibitors [3-8]. In humans, it is expressed primarily in the liver [9]. Glyoxylate, a toxic compound, can be detoxified to glycine by alanine-glyoxylate transaminase (AGT) in the peroxisome; in the cytosol, it can be reduced back to glycolate by glyoxylate-hydroxy pyruvate reductase (GR/HPR) or oxidised to oxalate by an NAD^+-dependent lactate dehydrogenase. Genetic deficiencies of AGT or GR/HPR lead to primary hyperoxaluria type I and type II, respectively, diseases characterized by the accumulation of calcium oxalate stones, in the kidneys in particular [10]. In mammals, the pig liver enzyme [11-14] and the one from human liver as well as its recombinant form (hGOX) were characterized at the molecular level [15-20].

Abbreviations
DCIP, dichlorophenol indophenol; F3Lac, trifluorolactate; Fcb2, flavocytochrome b_2; FMN, flavin mononucleotide; hGOX, human glycolate oxidase; LCHAO, long-chain hydroxy acid oxidase; LMO, lactate monooxygenase from *M. smegmatis* (formerly called lactate oxidase); LOX, lactate oxidase from *A. viridans*; MD, molecular dynamics; MDH, mandelate dehydrogenase; QM/MM, quantum mechanics/molecular mechanics; sGOX, spinach glycolate oxidase.

FEBS Open Bio **13** (2023) 938–950 © 2022 The Authors. *FEBS Open Bio* published by John Wiley & Sons Ltd on behalf of Federation of European Biochemical Societies.

Glycolate oxidase is a member of the family of FMN-dependent L-2-hydroxy acid-oxidizing enzymes. Other well-characterized members include its isozyme B (long-chain hydroxy acid oxidase, LCHAO or HAOX2), as well as microbial lactate oxidase (LOX) and lactate monooxygenase (LMO); dehydrogenases-electron transferases such as flavocytochrome b_2 (Fcb2, an L-lactate cytochrome *c* oxido-reductase) and mandelate dehydrogenases (MDH) have also been characterized. Crystal structures of these enzymes show a well-conserved $\beta_8\alpha_8$ barrel with FMN bound at its C-terminal end [3,4,5,7,21,22,23,24,25]. Active site residues are also well conserved, with a few substitutions due to different substrate specificity. As loop 4, between β-strand 4 and α-helix 4, is flexible, the full loop is not always visible in crystal structures. Depending on the ligand in the active site, or even between subunits in the same crystal unit, the visible length can be different or have a different conformation [16,17,22,23,24,25,26,27,28,29,30,31,32,33]. These structures, combined with results from solution studies [30-37], show that loop 4 contributes to catalysis. A few residues in or close to the active site pocket also display mobility, such as W110 in hGOX [16] and its homologue W108 in sGOX [6] or invariant R164 in sGOX [7] and its homologue R289 in Fcb2 [38] (Fig. 1). This mobility does not facilitate understanding the side chains mechanistic role. The case of W110 (108) is particularly interesting. This residue, which is unique to glycolate oxidases at this position in the family, is close to the active site. The W108S variant of sGOX had a 500-fold lower k_{cat} and a strikingly higher K_m for glycolate compared to the WT [6]. It was concluded that this residue may play a role in substrate specificity. Indeed, for the spinach and the human enzyme, crystal structures of complexes with several inhibitors showed an adaptation of the side-chain conformation which in some cases even induced movements of other residues extending to loop 4 [7,16].

Three possible chemical mechanisms were considered for the oxidation of a carbon–hydrogen bond by these enzymes, namely a hydride transfer mechanism, a proton/electron mechanism and a carbanion mechanism [39,40]. Experimental evidence in favour of the substrate α-hydrogen abstraction as a proton, followed by electron transfer from the carbanion to the flavin, had been proposed early on for LMO [41]. When the first crystal structures became available, the active site base was identified as a histidine (H260 in hGOX and H373 in Fcb2) (Fig. 1). Substrate modelling, starting from the pyruvate molecule orientation in Fcb2 crystals [21] suggested two possible substrate-binding modes [42,43]. In the first one, the C2 hydrogen was pointing towards the catalytic histidine N3, ready for abstraction as a proton, with formation of a carbanion (Fig. S1A); in the second one, obtained by a 40° rotation of the substrate C1–C2 bond, the catalytic histidine N3 was hydrogen bonded to the substrate hydroxyl group, orienting the lactate C2 hydrogen towards flavin N5 for a hydride transfer (Fig. S1B).

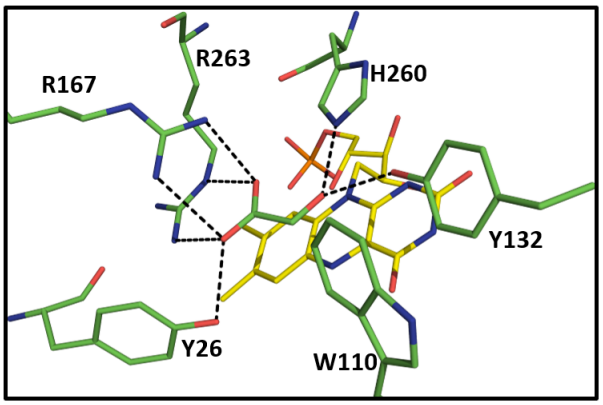

Fig. 1. hGOX active site with bound glyoxylate, drawn from the crystal structure (Protein Data Bank 2RDU). Atom colouring: red for oxygen, blue for nitrogen, yellow for the flavin carbon atoms and green for the other amino acids and glyoxylate. The side chains in the figure are conserved in other family members, except for Y26 (phenylalanine in LCHAO) and, importantly, for W110 which is specific to GOX; in other family members, it is replaced by a variety of residues. The hydrogen bonds and other close interaction are shown by dotted lines, as described in [16]. Glyoxylate is here in its unhydrated form and can be considered as playing the role of an inhibitor. In the Fcb2 crystal structure with bound pyruvate (Protein Data Bank 1FCB), the hydrogen bonding interactions are identical to those shown here, with the exception that here mobile hGOX R167 is in the so-called proximal position and interacts with the ligand carboxylate, while its Fcb2 homologue R289 is in the so-called distal position (Fig. S1), interacting with D292, an invariant residue in the family [21]. In the 1FCB Fcb2 structure, the flavin is in the semiquinone state [21,62] in agreement with the evidence that pyruvate stabilizes the flavin semiquinone [63].

Numerous studies have tried to understand the role of active site residues in catalysis and to solve the mechanistic issue, using combinations of site-directed mutagenesis, kinetic studies (with a variety of substrates and inhibitors) including solvent and pH effects, primary kinetic isotope effects as well as crystallography. MD and QM/MM computations were also carried out on a minimal model of the Fcb2 active site [44], on its whole flavodehydrogenase domain [45] and on LCHAO [46]. In some cases, experimental results led to ambiguous conclusions. But in other cases, pieces of evidence were provided that are hardly compatible or even incompatible with a hydride transfer mechanism [43,47,48,49,50,51,52,53,54,55,56,57].

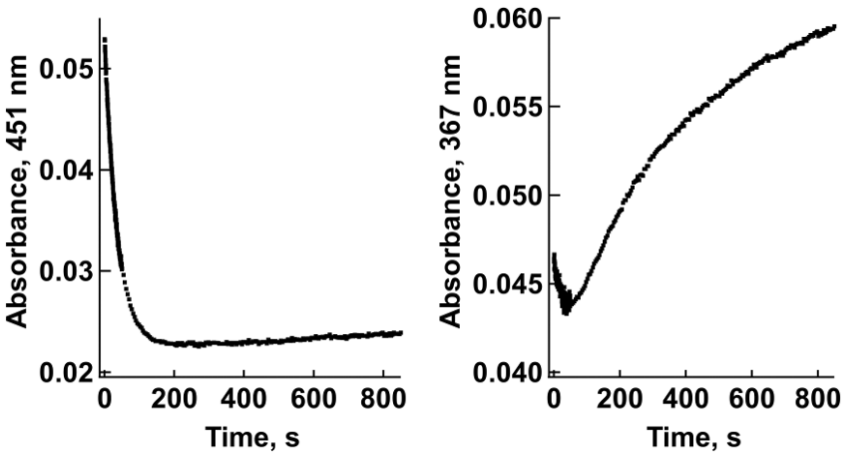

Fig. 2. Evolution of the absorbance at 451 nm (left) and 367 nm (right) upon hGOX reduction by DL-F3Lac (3.9 mM). Similar traces were obtained with glycolate and lactate (Figs S2 and S3). For more details, see Materials and methods.

In this work, we analyse the reactivity of trifluorolactate (F3Lac) with hGOX, and compare it to that of lactate and glycolate. It is expected that electron attraction by the three fluorine atoms will impede the C2 hydrogen removal as a hydride ion. Indeed, F3Lac has been shown not to be a substrate but an inhibitor of NAD-dependent lactate dehydrogenases from four different species [58-61]. We recently showed that F3Lac is a substrate for Fcb2 [49]. Here, we show that F3Lac is also a substrate for glycolate oxidase, another piece of evidence pointing to a carbanion mechanism.

Results

We have compared the reactivity of hGOX with three α-hydroxy acids, glycolate, L-lactate and trifluorolactate (F3Lac). The latter had never been tested with this enzyme and the present work demonstrates that it is a substrate. This has important mechanistic consequences. Moreover, for the three substrates, we report a phenomenon which had never been observed previously, namely the formation of a flavin semiquinone by an electron transfer between a reduced and an oxidized flavin during the reduction process.

Unexpected flavin semiquinone formation after reduction

The time course of flavin reduction by glycolate, L-lactate and DL-F3Lac was monitored over several hundred seconds using a diode array stopped-flow spectrophotometer under anaerobic conditions, as detailed in Materials and methods. For the three substrates, the initial absorption spectrum was consistent with that of the oxidized flavin form (Fig. 3). Analysis of the absorbance changes versus time at 451 and 367 nm (close to the two maxima of the oxidized flavin spectrum) pointed out at least two kinetic phases. At 451 nm, the absorbance started decreasing with time in a nearly monoexponential mode (Fig. 2, left; Figs S2 and S3 for glycolate and lactate); at longer times, from a few seconds for glycolate to a few dozen seconds for DL-F3Lac, a second increasing phase of low amplitude appeared. At 367 nm (Fig. 2, right; Figs S2 and S3), the initial phase of decreasing absorbance corresponding to flavin reduction was followed by an absorbance increase of higher amplitude. This second phase, ascribed to formation of a flavin semiquinone, suggested a one-electron transfer from a reduced flavin to an oxidized one. In other words, the flavin reduced form was not the final product of the reaction, but an intermediate. Altogether, the end spectrum was not that of reduced flavin, but that of the anionic flavin semiquinone (Fig. 3).

Determination of rate constants

For determining the rate constants, in order to avoid simplifying approximations, we globally fitted the total time course of the transients from a few milliseconds to several hundred seconds using numerical data analysis. This provided the evaluation of the dependence on substrate concentration of all the rate constants involved in the formation of the flavin semiquinone. For each substrate, the spectra of the different species were averaged over the spectra derived from the global fit, regardless of the substrate concentration.

The question was whether the interflavin electron transfer was taking place within a tetramer or between

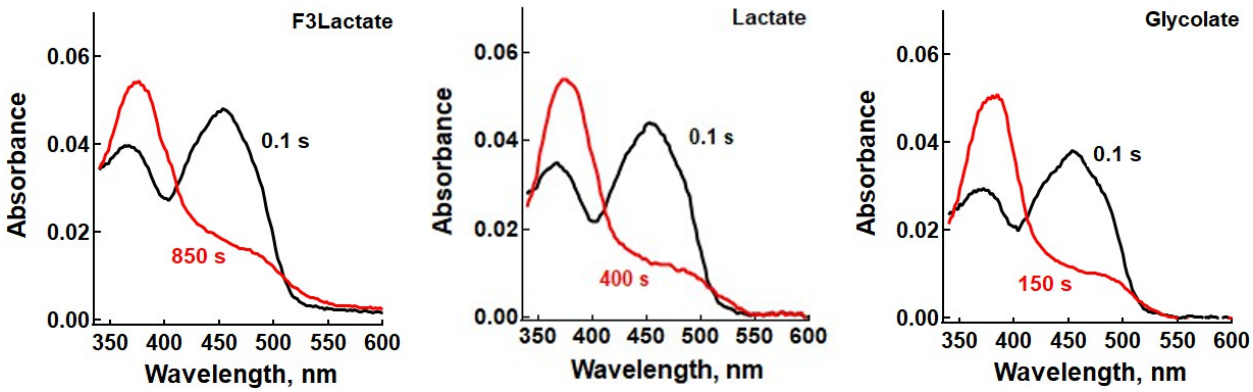

Fig. 3. First and last spectra recorded during enzyme reduction by 3.9 mM DL-F3Lac, 5 mM L-lactate and 5 mM glycolate.

tetramers. Each dataset was fitted by distinct mechanisms assuming an electron transfer either between two different tetramers or between two subunits in the same tetramer. Whatever the substrate and its concentration, for mechanisms involving an inter-tetramers electron transfer, the quality of the fits was better than for those involving intra-tetramer electron transfer. In the following, only the results obtained by fitting the data with the inter-tetramers mechanism are presented and discussed. In the Supporting Information, Figs S5–S7 compare the fits assuming either an intra-tetramer or an inter-tetramers electron transfer for the three substrates.

For lactate and F3Lac, the inter-tetramers mechanism A was used as the kinetic model to globally fit the datasets.

Mechanism A

$$\mathrm{FMNox} + \mathrm{Sred} \underset{k_2}{\overset{k_1}{\rightleftarrows}} \mathrm{FMNox\text{-}Sred} \underset{k_{r3}}{\overset{k_3}{\rightleftarrows}} \mathrm{FMNred} + \mathrm{Sox}$$

Step *1* Step *2*

$$\mathrm{FMNox} + \mathrm{FMNred} \xrightarrow[\text{Step } 3]{k_4} 2\,\mathrm{FMNsq}$$

The reversibility of the flavin reduction step (step 2) had to be introduced in order to enable the formation of a flavin semiquinone at long times in combination with flavin reduction. Indeed, the absence of reversibility in step 2 favours the accumulation of the reduced form over time, limiting flavin semiquinone formation (Fig. S4). This reversibility is supported by the examination of the residuals which clearly showed that the model without reversibility was not appropriate and did not allow to fit the data (Fig. S5A). The introduction of reversibility in step 2 significantly decreased the value of the AIC criterion (definition in Materials and methods) and improved the quality of the global fit resulting in small, evenly distributed residuals (Fig. S5B). The introduction of reversibility is supported by published results showing that Fcb2, when reduced in anaerobiosis by lactate in excess, can reduce ketoacids such as halogeno pyruvates [48,50] (Scheme S1). This capacity was confirmed for hGOX (unpublished experiments) and LCHAO [64]. Similarly, it was shown that reduced MDH from *Pseudomonas putida* can reduce its normal product benzoylformate [27,55].

Mechanism A enabled an accurate description of the data obtained with F3Lac (Fig. S5) and lactate (Fig. S6). In contrast, it failed to provide good fits for glycolate (Fig. S7). In this case, the reactions of the inter-tetramers mechanism B were used as the kinetic model for the global analysis.

Mechanism B

$$\mathrm{FMNox} + \mathrm{Sred} \underset{k_2}{\overset{k_1}{\rightleftarrows}} \mathrm{FMNox\text{-}Sred} \underset{k_{r3}}{\overset{k_3}{\rightleftarrows}} \mathrm{FMNred\text{-}Sox} \underset{k_{r5}}{\overset{k_5}{\rightleftarrows}} \mathrm{FMNred} + \mathrm{Sox}$$

Step *1* Step *2* Step *3*

$$\mathrm{FMNox} + \mathrm{FMNred} \xrightarrow[\text{Step } 4]{k_4} 2\,\mathrm{FMNsq}$$

For this substrate, an additional reversibility step had to be added for the dissociation of the FMNred-

Sox complex; this suggests that this product of the physiological substrate has a higher affinity for the active site than have the products of lactate and F3Lac oxidation. This is supported by the crystallization of an hGOX-glyoxylate complex when the enzyme was mixed with glycolate under proper conditions [16]. The introduction of an intermediate species in the kinetic model clearly improves the residuals, and mechanism B satisfactorily matches the data (Fig. S7). The decrease in AIC value (see definition in Materials and methods), in spite of the increase in the number of parameters to be fitted, underlines the significant improvement in the quality of the fit to mechanism B for glycolate compared to mechanism A.

Altogether, the fact that the data are better fitted with the inter-tetramers than with the intra-tetramer mechanism is consistent with the fact that the distance between the flavin N5 atoms in adjacent subunits is on the order of 45 Å, a distance which makes the intra-tetramer electron transfer less likely. The dependence of the estimated kinetic parameters on substrate concentration for an electron transfer between tetramers is shown in Fig. 4 for F3Lac and in Figs S8 and S9 for glycolate and lactate respectively. Flavin reduction (k_3) follows the expected saturation curve; k_{r3} also reaches a plateau at high substrate concentrations. The derived enzymatic parameters for flavin reduction and semiquinone formation are given in Table 1. Altogether, F3Lac is about 10-fold slower than lactate, and 3- to 4-fold less efficient. But lactate itself is a 30-fold slower reductant than glycolate, and is 1.4×10^3-fold less efficient. The rate of FMNsq formation (k_4) increases linearly with substrate concentration and is 10-fold slower for F3Lac than for lactate. This parameter appears to depend essentially on the rate of FMNred formation.

The global fit allowed to reconstruct the shape of the absorption spectra of the three species involved (Fig. 5; Figs S10 and S11). It was checked that the shape of these spectra did not depend significantly on substrate concentration. Within experimental error, they correspond satisfactorily to the experimental ones, as well as to those reported in the literature. In particular, the reconstituted flavin semiquinone spectrum shows the same slight red shift in the 360–370 nm region compared to the low-wavelength maximum of the oxidized species; it also has the shoulder in the 480–500 nm region, typical of the flavin anionic semiquinone spectrum (Fig. 3). This spectrum is similar to that of sGOX produced by photoreduction [65] and of the pig liver GOX produced by coulometric titration [14].

Discussion

By characterizing the reactivity of F3Lac as a substrate for GOX, this work provides important mechanistic information concerning the oxidation of L-2-hydroxy acids by glycolate oxidase, information which can be extended to other members of its family, as will be discussed later. But this work also describes the unexpected formation of a flavin semiquinone, which will be discussed first.

Flavin semiquinone formation

Under our reaction conditions (anaerobiosis at pH 7 and 30 °C), the semiquinone was formed by electron transfer between a reduced flavin and an oxidized one, whatever the substrate. This phenomenon has never been reported for the physiological substrate glycolate. It was not observed with the spinach enzyme, at pH

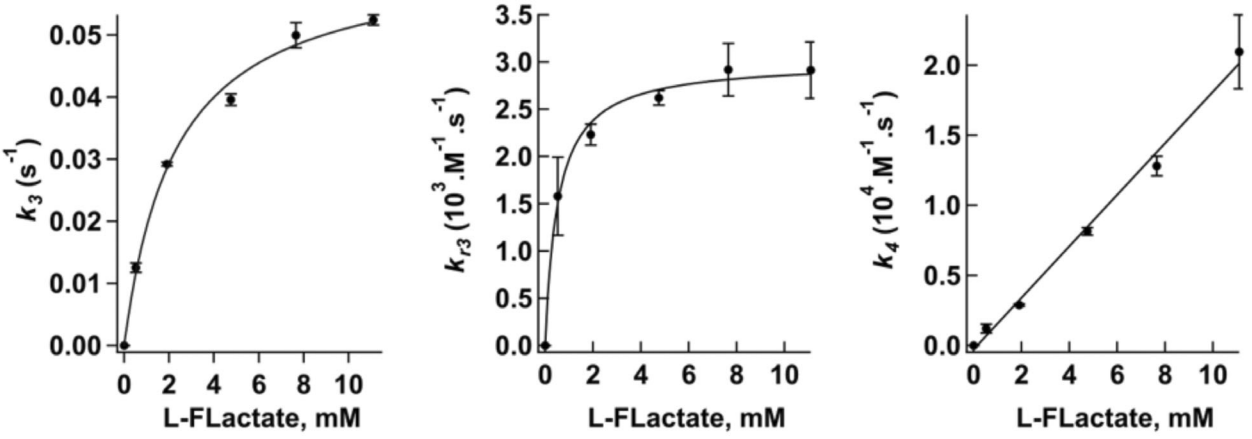

Fig. 4. Dependence of the kinetic parameters on F3Lac concentration. The experiments were carried out with the racemic F3Lac but the results are expressed in terms of the L-stereoisomer concentration. Error bars represent the standard deviations (SD).

Table 1. Kinetic parameters for flavin reduction and semiquinone formation by glycolate, L-lactate and F3Lac. The values given here were calculated using the rates obtained by computer simulation of the experimental traces at the various substrate concentrations, as shown in Fig. 4 and Figs S8 and S9.

	k_3		k_{r3}		k_4	k_5		k_{r5}	
Substrate	k_{max} (s^{-1})	$K_{1/2}$ (mM)	k_{max} (s^{-1})	$K_{1/2}$ (mM)	Slope (s^{-1}·mM^{-2})	k_{max} (s^{-1})	$K_{1/2}$ (mM)	k_{max} (s^{-1})	$K_{1/2}$ (mM)
Glycolate	25.05 ± 0.45	0.195 ± 0.020	6.83 ± 0.50	1.04 ± 0.22	$654 \times 10^6 \pm 64 \times 10^6$	0.11 ± 0.02	0.67 ± 0.42	22 270 ± 204	ND
Lactate	0.78 ± 0.05	8.35 ± 1.44	5037 ± 388	1.99 ± 0.55	$18.0 \times 10^6 \pm 2.4 \times 10^6$				
F3Lac[a]	0.063 ± 0.003	2.29 ± 0.03	3008 ± 80	0.53 ± 0.08	$1.84 \times 10^6 \pm 0.08 \times 10^6$				

[a]Results expressed in terms of the L-stereoisomer.

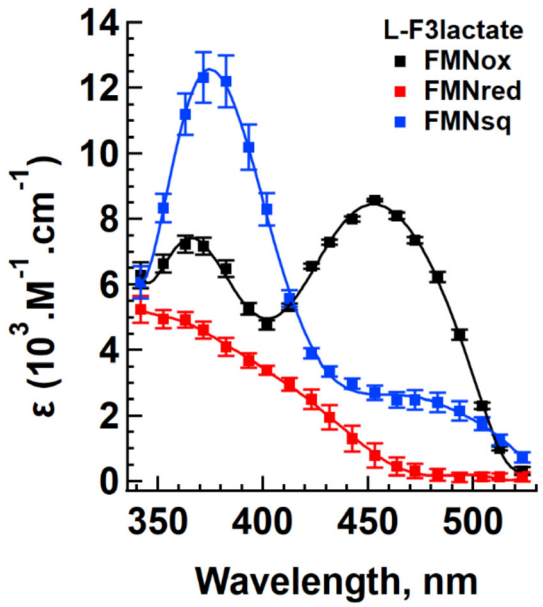

Fig. 5. Reaction with DL-F3lactate: calculated spectra of the three redox states resulting from the global analysis of the experimental data. For the reactions with glycolate and lactate, the spectra are given in Figs S10 and S11. Error bars represent the standard deviations (SD).

8.3 and 4 °C after 10 min in a diode array spectrophotometer [65]. Using a 100 mM phosphate buffer but at pH 7 and 30 °C as in the present work, Pennati and Gadda [19] did not identify the phenomenon when monitoring hGOX reduction over 1 s at 450 nm. The existence of a slow phase of small amplitude at the end of their observation time can possibly be interpreted as indicating incipient semiquinone formation.

In itself, the phenomenon suggests that the redox potential values of the $E.FMN_{red}/E.FMN_{sq}$ and $E.FMN_{sq}/E.FMN_{ox}$ couples are close. For the pig liver enzyme at pH 7.1 and 10 °C in 100 mM phosphate buffer, they were determined to be – 30 mV and −17 mV respectively [14]. There is about 92% sequence identity between the pig liver and the human enzyme; the crystal structure of the latter (Protein Data Bank 2NZL for ex.) indicates that all the substitutions are located on the surface, except one which is not close to the flavin. Thus, one may assume that the human enzyme has similar redox potentials at the same pH in our 50 mM phosphate buffer at 30 °C.

About the chemical mechanism of substrate oxidation

Our experimental results show that replacing the lactate CH_3 group by the electron attracting CF_3 group

does not prevent F3Lac from being a substrate for glycolate oxidase. This is in stark contrast with the fact that F3Lac is an inhibitor for several NAD-dependent lactate dehydrogenases [58-61]. Similarly, trifluoroethanol is known as an inhibitor of NAD-dependent alcohol dehydrogenases [66-69]. Numerous studies with these enzymes from horse liver and yeast have used this compound in solution as a ligand and inhibitor [70-73]. Another example of the negative effect of the CF_3 group in a hydride transfer mechanism is that of trifluoroalanine, which was co-crystallized with D-amino acid oxidase as an inhibitor, while alanine is a substrate for this enzyme [74,75]. In contrast, the facilitating effect of the fluorines in the formation of a carbanion is illustrated by the case of mandelate racemase. For this enzyme, lactate is an inhibitor, while F3Lac is a substrate and can be racemized [76,77].

In view of this facilitating effect of the fluorine atoms in a carbanion mechanism, a faster rate and a higher catalytic efficiency for F3Lac compared to lactate could have been expected (Table 1). In our previous work with Fcb2 for the same lactate/F3Lac comparison [49], the difference between the two substrates was much larger (about four orders of magnitude for the rate). But in that case, the F3Lac catalytic efficiency was still higher than that of mandelate, a very poor Fcb2 substrate [43,49]. The F3Lac low rate and efficiency can possibly arise from several factors: a steric problem due to the replacement of the methyl group by the trifluoromethyl group (lactate itself is a poor substrate compared to glycolate, Table 1), a possible distortion of substrate binding or transition state geometry due to potential halogen bonds and, importantly, a higher redox potential of the F3Lac/F3Pyr couple compared to the lactate/pyruvate couple. The Lac/Pyr couple redox potential is −190 mV, that of the glycolate/glyoxylate couple is −87 mV at pH 7 [78] and that of the F3Lac/F3Pyr couple is on the order of −60 mV [49]. Thus, the redox potential differences between hGOX (E_m = −68 mV for the pig liver enzyme [14]) and those substrates suggest that the driving force for reduction by F3Lac is less than that for lactate. This may counteract the favourable effect of the fluorines on C2 proton abstraction. Another important but unpredictable factor is the role of side chains mobility, in particular that of W110, and of loop 4, as observed in several crystal structures [7,16,17] (see Introduction).

The literature provides several other pieces of evidence in favour of the carbanion mechanism for this enzyme family, evidence that cannot be rationalized by a hydride transfer mechanism [79]. One example is the formation by LMO of a catalytically competent covalent intermediate between FMN and glycolate [53,54], formed by attack of a carbanion on the electron-deficient oxidized flavin N5. No catalytic adduct has been detected with other family members; it could be that the formation of covalent intermediates during the oxidation of normal substrates is sterically difficult. With MDH, another important piece of evidence (among others) in favour of a carbanion mechanism is the formation, on the way to flavin reduction by the substrate at low temperature, of a transient spectral intermediate formed between an electron-rich donor (such as a carbanion) and electrophilic FMNox [55].

Another example is the different reactivity of mandelate for enzymes of the family. Modelling studies on the Fcb2 active site of its very slow substrate mandelate suggest that it can only bind as for a hydride mechanism due to steric interference, in particular by A198 (hGOX A81) and L230 (hGOX W110) [42,43,80]. Thus, when both lactate and mandelate appear to bind well to Fcb2 for hydride transfer, why is mandelate such a poor substrate for this enzyme? Variants with smaller residues at these positions and at homologous ones in family members increase the mandelate oxidation rate significantly [31,51,81,82,83]. Moreover, *bona fide* mandelate dehydrogenases have smaller residues at these positions and increasing their size decreases the activity for mandelate [84,85].

Further evidence in favour of a carbanion mechanism is provided by the dehydrohalogenation reaction of β-halogenated substrates catalysed by several family members (LMO, Fcb2 and LCHAO) [41,64,86]. This reaction does not in itself constitute an absolute proof. Indeed, it was suggested that halogen elimination could occur after enzyme reduction, when a hydride would displace the halogen from the normal keto acid product, as has been shown for D-amino acid oxidase [87]. However, a number of studies on Fcb2 WT and variant forms provided significant mechanistic information. These studies, carried out under transhydrogenation conditions (details in Scheme S1) between, for example, lactate and bromopyruvate, showed an isotope transfer from 2-(^{2}H)-lactate or 2-(^{3}H)-lactate to the products bromolactate and pyruvate [42,50,57,88]. An inverse deuterium isotope effect was determined for bromide elimination by the WT enzyme and several variant forms [42,50,56,57]. This can only result from an intermediate carbanion partitioning between isotope-insensitive elimination and isotope-sensitive protonation (Scheme S1). This inverse isotope effect is totally incompatible with a bromide displacement by a hydride from reduced flavin N5H.

Still more evidence is provided by the different reactivity of β-acetylenic substrates [89-94] or nitroethane [95-97] between GOX family members and D-amino acid oxidase, which works by hydride transfer [98,99].

In spite of all the evidence briefly summarized here (more evidence is discussed in [79]), hydride transfer was proposed in recent years on the basis of kinetic isotope effects on Fcb2 variant forms [100,101], of the interpretation of crystal structures [83,100,102] and of the results of QM and QMM studies on Fcb2 [44,45] and on LCHAO [46]. A critical analysis of the validity of the interpretations in several of these papers can be found in [22,49,52,79].

Altogether, after the demonstration brought by the present results added to those obtained on Fcb2 with F3Lac [49], plus all the evidence briefly recalled above for other members of the family, can one still object to a carbanion mechanism for the FMN-dependent enzymes that oxidize L-2-hydroxy acids?

Materials and methods

Materials

DL-Trifluorolactate (DL-F3Lac) was obtained by chemical reduction of commercial ethyl-trifluoropyruvate with $NaBH_4$, followed by hydrolysis of the ethyl ester [103]. The compound purity and structure were analysed by gas chromatography, mass spectrometry and nuclear magnetic resonance. The concentration of stock solutions was determined on an HPLC cation exchange column (AMINEX HPX 87H; BioRad, Hercules, CA, USA) developed at 30 °C with 5 mM sulfuric acid at 0.3 mL·min^{-1}. The elution profile was monitored at 210 nm. The same system was used for identifying the oxidation product, trifluoropyruvic acid, by comparison with a commercial sample. The L-lactate lithium salt, trifluoropyruvic acid, protocatechuate dioxygenase and protocatechuic acid were purchased from Sigma (St. Louis, MO, USA). All other chemicals were of analytical grade. Recombinant hGOX was expressed and purified as described [15]. It was used without cleavage of the His-tag at the N terminus.

Methods

The enzyme concentration was determined in terms of its flavin content (ε_{452} = 8.6 mM^{-1}·cm^{-1}) [15]. The working buffer was 50 mM Na^+/K^+ phosphate buffer pH 7. For experiments in anaerobiosis, buffers and substrate solutions were purged by bubbling with argon from which oxygen had been scrubbed by an Alltech Big Oxygen Trap. The concentrated enzyme was separately ventilated without bubbling, and finally, diluted with the relevant deaerated buffer. A small volume (~ 1%) of 40 mM protocatechuate was added to the solutions during deaeration. Before introducing enzyme and reagents into the stopped-flow spectrophotometer, a small volume (~ 1%) of protocatechuate dioxygenase (6.10^{-3} units·mL^{-1}) was added to the solutions, as proposed by Patil and Ballou [104]. After mixing with substrate, the enzyme concentration was on the order of 5–6 μM. The absorption spectra and their evolution over time were followed with an Applied Photophysics SX20 (Applied Photophysics Limited, Leatherhead, UK) stopped-flow spectrophotometer equipped with a diode array detector.

Global fit analysis

Prior to the analysis of the selected absorption spectra, a baseline correction was performed in order to eliminate the instrumental drift over time. The kinetics of absorbance evolution over time were analysed at 19 wavelengths between 340 and 520 nm, at intervals of 10 nm. Each dataset consisting of these 19 series of traces was globally fitted according to mechanisms A, B, IntraA and IntraB. The associated differential rate laws are given in the Supporting Information. The global analysis was performed using MATHEMATICA software (Version 13.0, 2021; Wolfram Research, Inc., Champaign, IL, USA). The MultiNonlinearModelFit function was used to fit the data by numerically solving the differential equations and sharing the different wavelength-independent rate constant parameters, while the molar extinction coefficients of the different species were estimated for each wavelength. The initial values of all parameters were chosen arbitrarily, except for the rate constants k_1 and k_2 associated with step 1 of the FMNox-Sred complex formation (see equations in Results and, in Supporting Information, Global fit analysis and equations section). They were set to $k_1 = 30.10^6$ M^{-1}·s^{-1} and k_2 = 450 s^{-1} for glycolate and $k_1 = 156.10^3$ M^{-1}·s^{-1} and k_2 = 200 s^{-1} for lactate and DL-F3Lac. The substrate concentration was introduced as an initial parameter. We assumed that the FMNox and FMNox-Sred species exhibited the same absorption spectrum. The quality of the fit was judged by the visual inspection of the plots of residuals. Furthermore, in order to evaluate the suitability of the different kinetic models in describing the data and to identify the one that led to the best compromise between the quality of the fit and the number of parameters to be fitted, we used the Akaike information criterion (AIC). As the number of degrees of freedom (i.e. the number of parameters) are different between the kinetic models, AIC allows to compare the models and to estimate the relevance of the improvement of the fit following an increase in the number of parameters. The value of AIC was estimated according to the following equation

$$\mathrm{AIC} = N \cdot \ln\left(\frac{\mathrm{SSQ}}{N}\right) + 2 \cdot (p+1),$$

where N designates the number of data points, SSQ the sum of squares and p the number of parameters to be fitted. For each dataset, the best kinetic model chosen will be the one with the lowest AIC value.

For each substrate concentration, all rate constants presented in this work are an average value of the rate constants estimated from the global analysis of at least three datasets.

Acknowledgements

The authors are grateful to Prof C. Houée Levin, Prof P. de Oliveira and Dr Pascal Pernot for fruitful discussions and advice. This work was supported by recurrent academic funding from the CNRS and Université Paris-Sud (now renamed Université Paris-Saclay).

Conflict of interest

The authors declare no conflict of interest.

Data accessibility

Figure 1: drawn from the Protein Data Bank (PDB) structure, code HAOX1_human, Q9UJM8 and from https://doi.org/10.1021/bi701710r. The structures corresponding to the codes given at the end of the Supporting Information are all found in the PDB. The rest of the experimental data (individual stopped-flow recordings) are available on request from the authors.

Author contributions

FL conceived the work and carried out the experiments; HP proposed the kinetic models and carried out data analysis; FL and HP contributed to manuscript writing.

References

1 Kun E, Dechary JM, Pitot HC. The oxidation of glycolic acid by a liver enzyme. *J Biol Chem*. 1954;**210**:269–80.
2 Richardson KE, Tolbert NE. Oxidation of glyoxylic acid to oxalic acid by glycolic acid oxidase. *J Biol Chem*. 1961;**236**:1280–4.
3 Lindqvist Y, Brändén CI. The active site of spinach glycolate oxidase. *J Biol Chem*. 1989;**264**:3624–8.
4 Lindqvist Y. Refined structure of spinach glycolate oxidase at 2 Å resolution. *J Mol Biol*. 1989;**209**:151–66.
5 Lindqvist Y. Structure and mechanism of glycolate oxidase. In: Müller F, editor. *Chemistry and biochemistry of flavoenzymes*. Boca Raton: CRC Press; 1992. p. 367–87.
6 Stenberg K, Clausen T, Lindqvist Y, Macheroux P. Involvement of Tyr24 and Trp108 in substrate binding and substrate specificity of glycolate oxidase. *Eur J Biochem*. 1995;**228**:408–16.
7 Stenberg K, Lindqvist Y. Three-dimensional structures of glycolate oxidase with bound active-site inhibitors. *Protein Sci*. 1997;**6**:1009–15.
8 Macheroux P, Kieweg V, Massey V, Soderlind E, Stenberg K, Lindqvist Y. Role of tyrosine 129 in the active site of spinach glycolate oxidase. *Eur J Biochem*. 1993;**213**:1047–54.
9 Jones JM, Morrell JC, Gould SJ. Identification and characterization of HAOX1, HAOX2, and HAOX3, three human peroxisomal 2-hydroxy acid oxidases. *J Biol Chem*. 2000;**275**:12590–7.
10 Salido E, Pey AL, Rodriguez R, Lorenzo V. Primary hyperoxalurias: disorders of glyoxylate detoxification. *Biochim Biophys Acta*. 2012;**1822**:1453–64.
11 Schuman M, Massey V. Purification and characterization of glycolic acid oxidase from pig liver. *Biochim Biophys Acta*. 1971;**227**:500–20.
12 Schuman M, Massey V. Effect of anions on the catalytic activity of pig liver glycolic acid oxidase. *Biochim Biophys Acta*. 1971;**227**:521–37.
13 Schuman Jorns M. Glycolic acid oxidase from pig liver. *Methods Enzymol*. 1975;**41B**:337–43.
14 Pace C, Stankovich M. Oxidation-reduction properties of glycolate oxidase. *Biochemistry*. 1986;**25**:2516–22.
15 Vignaud C, Pietrancosta N, Williams EL, Rumsby G, Lederer F. Purification and characterization of recombinant human liver glycolate oxidase. *Arch Biochem Biophys*. 2007;**465**:410–6.
16 Murray MS, Holmes RP, Lowther WT. Active site and loop 4 movements within human glycolate oxidase: implications for substrate specificity and drug design. *Biochemistry*. 2008;**47**:2439–49.
17 Bourhis JM, Vignaud C, Pietrancosta N, Guéritte F, Guénard D, Lederer F, et al. Structure of human glycolate oxidase in complex with the inhibitor 4-carboxy-5-[(4-chlorophenyl)sulfanyl]-1,2,3-thiadiazole. *Acta Crystallogr Sect F Struct Biol Cryst Commun*. 2009;**65**:1246–53.
18 Schwam H, Michelson S, Randall WC, Sondey JM, Hirschmann R. Purification and characterization of human liver glycolate oxidase. Molecular weight, subunit, and kinetic properties. *Biochemistry*. 1979;**18**:2828–33.
19 Pennati A, Gadda G. Involvement of ionizable groups in catalysis of human liver glycolate oxidase. *J Biol Chem*. 2009;**284**:31214–22.
20 Pennati A, Gadda G. Stabilization of an intermediate in the oxidative half reaction of human liver glycolate oxidase. *Biochemistry*. 2011;**50**:1–3.
21 Xia ZX, Mathews FS. Molecular structure of flavocytochrome b_2 at 2.4 Å resolution. *J Mol Biol*. 1990;**212**:837–63.

22 Cunane LM, Barton JD, Chen Z-W, Lê KHD, Amar D, Lederer F, et al. Crystal structure analysis of recombinant rat kidney long-chain α-hydroxy acid oxidase. *Biochemistry*. 2005;**44**:1521–31.
23 Sukumar N, Xu Y, Gatti DL, Mitra B, Mathews FS. Structure of an active soluble mutant of the membrane-associated (S)-mandelate dehydrogenase. *Biochemistry*. 2001;**40**:9870–8.
24 Leiros I, Wang E, Rasmussen T, Oksanen E, Repo H, Petersen SB, et al. The 2.1 Å structure of *Aerococcus viridans* L-lactate oxidase (LOX). *Acta Crystallogr Sect F Struct Biol Cryst Commun*. 2006;**62**:1185–90.
25 Kean KM, Karplus PA. Structure and role for active site lid of lactate monooxygenase from *Mycobacterium smegmatis*. *Protein Sci*. 2019;**28**:135–49.
26 Chen Z-C, Vignaud C, Jaafar A, Lévy B, Guéritte F, Guénard D, et al. High resolution crystal structure of rat long chain hydroxy acid oxidase in complex with the inhibitor 4-carboxy-5-[(4-chlorophenyl)sulfanyl]-1, 2, 3-thiadiazole. Implications for inhibitor specificity and drug design. *Biochimie*. 2012;**94**:1172–9.
27 Sukumar N, Dewanti AR, Mitra B, Mathews FS. High resolution structures of an oxidized and reduced flavoprotein: the water switch in a soluble form of (S)-mandelate dehydrogenase. *J Biol Chem*. 2004;**279**:3749–57.
28 Sukumar N, Dewanti A, Merli A, Rossi GL, Mitra B, Mathews FS. Structures of the G81A mutant form of the active chimera of (S)-mandelate dehydrogenase and its complex with two of its substrates. *Acta Crystallogr D Biol Crystallogr*. 2009;**65**:543–52.
29 Sukumar N, Liu S, Li W, Mathews FS, Mitra B, Kandavelu P. Structure of the monotopic membrane protein (S)-mandelate dehydrogenase at 2.2 Å resolution. *Biochimie*. 2018;**154**:45–54.
30 Li SJ, Umena Y, Yorita K, Matsuoka T, Kita A, Fukui K, et al. Crystallographic study on the interaction of L-lactate oxidase with pyruvate at 1.9 Å resolution. *Biochem Biophys Res Commun*. 2007;**358**:1002–7.
31 Stoisser T, Rainer D, Leitgeb S, Wilson DK, Nidetzky B. The Ala95-to-Gly substitution in *Aerococcus viridans* L-lactate oxidase revisited – structural consequences at the catalytic site and effect on reactivity with O_2 and other electron acceptors. *FEBS J*. 2015;**282**:562–78.
32 Stoisser T, Klimacek M, Wilson DK, Nidetzky B. Speeding up the product release: a second-sphere contribution from Tyr191 to the reactivity of L-lactate oxidase revealed in crystallographic and kinetic studies of site-directed variants. *FEBS J*. 2015;**282**:4130–40.
33 Stoisser T, Brunsteiner M, Wilson DK, Nidetzky B. Conformational flexibility related to enzyme activity: evidence for a dynamic active-site gatekeeper function of Tyr(215) in *Aerococcus viridans* lactate oxidase. *Sci Rep*. 2016;**6**:27892.
34 Ghrir R, Lederer F. Study of a zone highly sensitive to proteases in flavocytochrome b_2 from *Saccharomyces cerevisiae*. *Eur J Biochem*. 1981;**120**:279–87.
35 Reid GA, White S, Black MT, Lederer F, Mathews FS, Chapman SK. Probing the active site of flavocytochrome b_2 by site-directed mutagenesis. *Eur J Biochem*. 1988;**178**:329–33.
36 Belmouden A, Lederer F. The role of a β barrel loop 4 extension in modulating the physical and functional properties of long-chain 2-hydroxyacid oxidase isozymes. *Eur J Biochem*. 1996;**238**:790–8.
37 Pompon D, Iwatsubo M, Lederer F. Flavocytochrome b_2 (baker's yeast). Deuterium isotope effect studied by rapid-kinetic methods as a probe for the mechanism of electron transfer. *Eur J Biochem*. 1980;**104**:479–88.
38 Tegoni M, Cambillau C. The 2.6 Å refined structure of the *Escherichia coli* recombinant *Saccharomyces cerevisiae* flavocytochrome b_2-sulfite complex. *Protein Sci*. 1994;**3**:303–13.
39 Ghisla S. Dehydrogenation mechanism in flavoprotein catalysis. In: Massey V, Williams CH, editors. *Flavins and flavoproteins*. Amsterdam: Elsevier; 1982. p. 133–42.
40 Ghisla S, Massey V. Mechanisms of flavoprotein-catalyzed reactions. *Eur J Biochem*. 1989;**181**:1–17.
41 Walsh C, Lockridge O, Massey V, Abeles R. Studies on the mechanism of action of the flavoenzyme lactate oxidase. Oxidation and elimination with ß-chlorolactate. *J Biol Chem*. 1973;**248**:7049–54.
42 Dubois J, Chapman SK, Mathews FS, Reid GA, Lederer F. Substitution of Tyr254 with Phe at the active site of flavocytochrome b_2: consequences on catalysis of lactate dehydrogenation. *Biochemistry*. 1990;**29**:6393–400.
43 Gondry M, Dubois J, Terrier M, Lederer F. The catalytic role of tyrosine 254 in flavocytochrome b_2 (L-lactate dehydrogenase from baker's yeast) – comparison between the Y254F and Y254L mutant proteins. *Eur J Biochem*. 2001;**268**:4918–27.
44 Tabacchi G, Zucchini D, Caprini G, Gamba A, Lederer F, Vanoni MA, et al. L-lactate dehydrogenation in flavocytochrome b_2 – a first principles molecular dynamics study. *FEBS J*. 2009;**276**:2368–80.
45 Gillet N, Ruiz-Pernia JJ, de la Lande A, Levy B, Lederer F, Demachy I, et al. QM/MM study of L-lactate oxidation by flavocytochrome b_2. *Phys Chem Chem Phys*. 2016;**18**:15609–18.
46 Cao Y, Han S, Yu L, Qian H, Chen JZ. MD and QM/MM studies on long-chain L-α-hydroxy acid oxidase: substrate binding features and oxidation mechanism. *J Phys Chem B*. 2014;**118**:5406–17.
47 Gaume B, Sharp RE, Manson FDC, Chapman SK, Reid GA, Lederer F. Mutation to glutamine of

histidine 373, the catalytic base of flavocytochrome b_2 (L-lactate dehydrogenase). *Biochimie*. 1995;**77**:621–30.
48 Rao KS, Lederer F. About the *pK*a of the active-site histidine in flavocytochrome b_2 (yeast L-lactate dehydrogenase). *Protein Sci*. 1998;**7**:1531–7.
49 Lederer F, Vignaud C, North P, Bodevin S. Trifluorosubstrates as mechanistic probes for an FMN-dependent L-2-hydroxy acid-oxidizing enzyme. *Biochim Biophys Acta*. 2016;**1864**:1215–21.
50 Urban P, Lederer F. Intermolecular hydrogen transfer catalyzed by a flavodehydrogenase, bakers' yeast flavocytochrome b_2. *J Biol Chem*. 1985;**260**:11115–22.
51 Sinclair R, Reid GA, Chapman SK. Re-design of *Saccharomyces cerevisiae* flavocytochrome b_2: introduction of L-mandelate dehydrogenase activity. *Biochem J*. 1998;**333**:117–20.
52 Elhoul MB, Machillot P, Benoit M, Lederer F. Translational misreading, amino acid misincorporation and misinterpretations. The case of the flavocytochrome b_2 H373Q variant. *Biochim Biophys Acta*. 2017;**1865**:353–8.
53 Ghisla S, Massey V. Studies on the catalytic mechanism of lactate oxidase. Formation of enantiomeric flavin-N (5)-glycollyl adducts via carbanion intermediates. *J Biol Chem*. 1980;**255**:5688–96.
54 Massey V, Ghisla S, Kieschke K. Studies on the reaction mechanism of lactate oxidase. Formation of two covalent flavin-substrate adducts on reaction with glycollate. *J Biol Chem*. 1980;**255**:2796–806.
55 Dewanti AR, Mitra B. A transient intermediate in the reaction catalyzed by (*S*)-mandelate dehydrogenase from *Pseudomonas putida*. *Biochemistry*. 2003;**42**:12893–901.
56 Bodevin S. *Analyse mutationelle de la réaction de déshydrohalogénation catalysée par le flavocytochrome b_2 (L-lactate déshydogénase). Implications mécanistiques*. Orsay: Université Paris XI; 1999.
57 Bodevin S, Lederer F. On the mechanistic value of the dehydrogenation reaction of β-halogeno α-hydroxy acids catalysed by FMN-dependent hydroxy acid-oxidizing enzymes: a mutational analysis with flavocytochrome b_2. In: Ghisla S, Kroneck P, Macheroux P, Sund H, editors. *Flavins and flavoproteins 1999*. Berlin: Rudolf Weber; 1999. p. 463–6.
58 Burstein SH, Ringold HJ. ß,ß,ß-Trifluorolactic acid. *Can J Biochem*. 1961;**39**:1848–9.
59 Anderson SR, Florini JR, Vestling CS. Rat liver lactate dehydrogenase. 3. Kinetics and specificity. *J Biol Chem*. 1964;**239**:2991–7.
60 Pogolotti A Jr, Rupley JA. Binding of trifluorolactate to pig heart H4-lactate dehydrogenase. *Biochem Biophys Res Commun*. 1973;**55**:1214–9.
61 Clarke AR, Wilks HM, Barstow DA, Atkinson T, Chia WN, Holbrook JJ. An investigation of the contribution made by the carboxylate group of an active site histidine-aspartate couple to binding and catalysis in lactate dehydrogenase. *Biochemistry*. 1988;**27**:1617–22.
62 Lederer F. Shuttling between the solution and the crystal. In: Miller S, Hille R, Palfey B, editors. *Flavins and flavoproteins 2011*. Berkeley: Lulu.com; 2013. p. 3–18.
63 Tegoni M, Janot JM, Silvestrini MC, Brunori M, Labeyrie F. Modifications of redox equilibria with semiquinone stabilization upon pyruvate binding to L-lactate cytochrome *c* oxidoreductase. *Biochem Biophys Res Commun*. 1984;**118**:753–9.
64 Urban P, Chirat I, Lederer F. Rat kidney L-2-hydroxyacid oxidase. Structural and mechanistic comparison with flavocytochrome b_2 from baker's yeast. *Biochemistry*. 1988;**27**:7365–71.
65 Macheroux P, Massey V, Thiele DJ, Volokita M. Expression of spinach glycolate oxidase in *Saccharomyces cerevisiae*: purification and characterization. *Biochemistry*. 1991;**30**:4612–9.
66 Colby TD, Bahnson BJ, Chin JK, Klinman JP, Goldstein BM. Active site modifications in a double mutant of liver alcohol dehydrogenase: structural studies of two enzyme-ligand complexes. *Biochemistry*. 1998;**37**:9295–304.
67 Plapp BV, Ramaswamy S. Atomic-resolution structures of horse liver alcohol dehydrogenase with NAD(+) and fluoroalcohols define strained Michaelis complexes. *Biochemistry*. 2012;**51**:4035–48.
68 Yahashiri A, Rubach JK, Plapp BV. Effects of cavities at the nicotinamide binding site of liver alcohol dehydrogenase on structure, dynamics and catalysis. *Biochemistry*. 2014;**53**:881–94.
69 Plapp BV, Eklund H, Brändén CI. Crystallography of liver alcohol dehydrogenase complexed with substrates. *J Mol Biol*. 1978;**122**:23–32.
70 Shore JD, Gutfreund H, Brooks RL, Santiago D, Santiago P. Proton equilibria and kinetics in the liver alcohol dehydrogenase reaction mechanism. *Biochemistry*. 1974;**13**:4185–41891.
71 Wolfe JK, Weidig CF, Halvorson HR, Shore JD, Parker DM, Holbrook JJ. pH-dependent conformational states of horse liver alcohol dehydrogenase. *J Biol Chem*. 1977;**252**:433–6.
72 Dickenson CJ, Dickinson FM. Inhibition by ethanol, acetaldehyde and trifluoroethanol of reactions catalysed by yeast and horse liver alcohol dehydrogenases. *Biochem J*. 1978;**171**:613–27.
73 Kim K, Plapp BV. Substitution of cysteine-153 ligated to the catalytic zinc in yeast alcohol dehydrogenase with aspartic acid and analysis of mechanisms of related medium chain dehydrogenases. *Chem Biol Interact*. 2019;**302**:172–82.
74 Harris CM, Molla G, Pilone MS, Pollegioni L. Studies on the reaction mechanism of *Rhodotorula gracilis D-*

amino-acid oxidase. Role of the highly conserved Tyr-223 on substrate binding and catalysis. *J Biol Chem*. 1999;**274**:36233–40.
75 Umhau S, Pollegioni L, Molla G, Diederichs K, Welte W, Pilone MS, et al. The x-ray structure of *D*-amino acid oxidase at very high resolution identifies the chemical mechanism of flavin-dependent substrate dehydrogenation. *Proc Natl Acad Sci USA*. 2000;**97**:12463–8.
76 St Maurice M, Bearne SL. Hydrophobic nature of the active site of mandelate racemase. *Biochemistry*. 2004;**43**:2524–32.
77 Nagar M, Narmandakh A, Khalak Y, Bearne SL. Redefining the minimal substrate tolerance of mandelate racemase. Racemization of trifluorolactate. *Biochemistry*. 2011;**50**:8846–52.
78 Clark WM. *Oxidation-reduction potentials of organic compounds*. New York: Williams and Wilkins; 1960.
79 Lederer F, Amar D, Ould Boubacar AK, Vignaud C. Which mechanism for (S)-2-hydroxy acid-oxidizing flavoenzymes? A tale of a histidine and two protons. In: Nishino T, Miura R, Tanokura M, Fukui K, editors. *Flavins and flavoproteins 2005*. Tokyo: ArchiTect Inc.; 2005. p. 193–204.
80 Lederer F, Mathews FS. Mechanism of L-lactate dehydrogenation catalyzed by flavocytochrome b_2 from baker's yeast. In: Edmonson DE, McCormick DB, editors. *Flavins and flavoproteins*. New York: Walter de Gruyter & Co; 1987. p. 133–42.
81 Yorita K, Aki K, Ohkuma-Soyejima T, Kokubo T, Misaki H, Massey V. Conversion of L-lactate oxidase to a long chain α-hydroxyacid oxidase by site-directed mutagenesis of alanine 95 to glycine. *J Biol Chem*. 1996;**271**:28300–5.
82 Jiang T, Gao C, Dou P, Ma C, Kong J, Xu P. Rationally re-designed mutation of NAD-independent L-lactate dehydrogenase: high optical resolution of racemic mandelic acid by the engineered *Escherichia coli*. *Microb Cell Fact*. 2012;**11**:151.
83 Mowat CG, Wehenkel A, Green AJ, Walkinshaw MD, Reid GA, Chapman SK. Altered substrate specificity in flavocytochrome b_2: structural insights into the mechanism of L-lactate dehydrogenation. *Biochemistry*. 2004;**43**:9519–26.
84 Smékal O, Yasin M, Fewson CA, Reid GA, Chapman SK. L-mandelate dehydrogenase from *Rhodotorula graminis*: comparisons with the L-lactate dehydrogenase (flavocytochrome b_2) from *Saccharomyces cerevisiae*. *Biochem J*. 1993;**290**: 103–7.
85 Dewanti AR, Xu Y, Mitra B. Role of glycine 81 in (S)-mandelate dehydrogenase from *Pseudomonas putida* in substrate specificity and oxidase activity. *Biochemistry*. 2004;**43**:10692–700.
86 Urban P, Lederer F. Baker's yeast flavocytochrome b_2. A mechanistic study of the dehydrohalogenation reaction. *Eur J Biochem*. 1984;**144**:345–51.
87 Ghisla S, Pollegioni L, Molla G. Revisitation of the βCl-elimination reaction of D-amino acid oxidase. *J Biol Chem*. 2011;**286**:40987–98.
88 Gondry M, Lederer F. Functional properties of the histidine-aspartate ion pair of flavocytochrome b_2 (L-lactate dehydrogenase): substitution of Asp282 with asparagine. *Biochemistry*. 1996;**35**:8587–94.
89 Cromartie TH, Walsh C. Mechanistic studies on the rat kidney flavoenzyme L-α-hydroxy acid oxidase. *Biochemistry*. 1975;**14**:3482–9.
90 Schonbrunn A, Abeles RH, Walsh CT, Ghisla S, Ogata H, Massey V. The structure of the covalent flavin adduct formed between lactate oxidase and the suicide substrate 2-hydroxy-3-butynoate. *Biochemistry*. 1976;**15**:1798–807.
91 Jewess PJ, Kerr MW, Whitaker DP. Inhibition of glycollate oxidase from pea leaves. *FEBS Lett*. 1975;**53**:292–6.
92 Fendrich G, Ghisla S. Studies on glycollate oxidase from pea leaves. Determination of stereospecificity and mode of inhibition by α-hydroxybutynoate. *Biochim Biophys Acta*. 1982;**702**:242–8.
93 Pompon D, Lederer F. On the mechanism of flavin modification during inactivation of flavocytochrome b_2 from baker's yeast by acetylenic substrates. *Eur J Biochem*. 1985;**148**:145–54.
94 Lehoux IE, Mitra B. (*S*)-mandelate dehydrogenase from *Pseudomonas putida*: mechanistic studies with alternate substrates and pH and kinetic isotope effects. *Biochemistry*. 1999;**38**:5836–48.
95 Porter DJ, Voet JG, Bright HJ. Direct evidence for carbanions and covalent N5 -flavin-carbanion adducts as catalytic intermediates in the oxidation of nitroethane by *D*-amino acid oxidase. *J Biol Chem*. 1973;**248**:4400–16.
96 Alston TA, Porter DJ, Bright HJ. Suicide inactivation of D-amino acid oxidase by 1-chloro-1-nitroethane. *J Biol Chem*. 1983;**258**:1136–41.
97 Genet R, Lederer F. The carbanion of nitroethane is an inhibitor of, and not a substrate for flavocytochrome b_2 (L-(+)-lactate dehydrogenase). *Biochem J*. 1990;**266**:301–4.
98 Mattevi A, Vanoni MA, Todone F, Rizzi M, Teplyakov A, Coda A, et al. Crystal structure of D-amino acid oxidase: a case of active site mirror-image convergent evolution with flavocytochrome b_2. *Proc Natl Acad Sci USA*. 1996;**93**:7496–501.
99 Ghisla S, Pollegioni L. *D*-amino acid oxidase: still new lessons from a seventy year old flavoprotein. In: Nishino T, Miura R, Tanokura M, Fukui K, editors. *Flavins and flavoproteins 2005*. Tokyo: ArchiTect Inc.; 2005. p. 17–32.

100 Tsai CL, Gokulan K, Sobrado P, Sacchettini JC, Fitzpatrick PF. Mechanistic and structural studies of H373Q flavocytochrome b_2: effects of mutating the active site base. *Biochemistry*. 2007;**46**:7844–51.
101 Sobrado P, Fitzpatrick PF. Solvent and primary deuterium isotope effects show that lactate CH and OH bond cleavages are concerted in Y254F flavocytochrome b_2, consistent with a hydride transfer mechanism. *Biochemistry*. 2003;**42**:15208–14.
102 Furuichi M, Suzuki N, Dhakshnamoorhty B, Minagawa H, Yamagishi R, Watanabe Y, et al. X-ray structures of *Aerococcus viridans* lactate oxidase and its complex with D-lactate at pH 4.5 show an α-hydroxyacid oxidation mechanism. *J Mol Biol*. 2008;**378**:436–46.
103 von dem Bussche-Hünnefeld C, Cescato C, Seebach D. Simple access to (R)-3,3,3-trifluorolactic and (S)-3,3,3-trifluorolactic acid and to (R)-(trifluoromethyl)oxirane and (S)-(trifluoromethyl)oxirane. *Chem Ber*. 1992;**125**:2795–802.
104 Patil PV, Ballou DP. The use of protocatechuate dioxygenase for maintaining anaerobic conditions in biochemical experiments. *Anal Biochem*. 2000;**286**: 187–92.

Supporting information

Additional supporting information may be found online in the Supporting Information section at the end of the article.

Fig. S1. Substrate modelling from the pyruvate coordinates in the Fcb2 crystal structure 1FCB.

Fig. S2. Evolution of the absorbance at 451 nm and 367 nm upon hGOX reduction by 5 mM glycolate over 0.5 s and 1000 s.

Fig. S3. Evolution of the absorbance at 451 nm (left) and 367 nm (right) upon hGOX reduction by 5 mM L-lactate.

Fig. S4. Simulated time evolution of concentrations of FMNred and FMNsq as a function of kr3 (Mechanism A), for reduction with L-F3Lac.

Fig. S5. Global numerical analysis of the absorbance variation overtime at 19 wavelengths from 340 to 520 nm at intervals of 10 nm, upon hGOX reduction by 3.9 mM DL-F3Lac.

Fig. S6. Global numerical analysis of the absorbance variation overtime at 19 wavelengths from 340 to 520 nm, at intervals of 10 nm upon hGOX reduction by 10 mM L-Lactate.

Fig. S7. Global numerical analysis of the absorbance variation overtime at 19 wavelengths from 340 to 520 nm, at intervals of 10 nm upon hGOX reduction by 5 mM glycolate.

Fig. S8. Dependence of the kinetic parameters on glycolate concentration.

Fig. S9. Dependence of the kinetic parameters on lactate concentration.

Fig. S10. Reaction with glycolate: spectra of the three redox states resulting from the global analysis of the experimental data.

Fig. S11. Reaction with lactate: spectra of the three redox states resulting from the global analysis of the experimental data.

Scheme S1. Principle of the transhydrogenation reaction.

Data S1. Global fit analysis and equations.

Data S2. Codes of PDB crystal structures of ternary complexes of alcohol dehydrogenases with NAD^+ and trifluoroethanol.